Psychoneuroendocrinology 96 (2018) 42–51

Contents lists available at ScienceDirect

Psychoneuroendocrinology

journal homepage: www.elsevier.com/locate/psyneuen

Effects of testosterone administration on threat and escape anticipation in the orbitofrontal cortex

Sarah J. Heany[a], Richard A.I. Bethlehem[b], Jack van Honk[a,c,d], Peter A. Bos[d], Dan J. Stein[a,e], David Terburg[a,d,*]

[a] Department of Psychiatry and Mental Health, University of Cape Town, South Africa
[b] Autism Research Centre, Department of Psychiatry, University of Cambridge, United Kingdom
[c] Institute of Infectious Diseases and Molecular Medicine, University of Cape Town, South Africa
[d] Department of Experimental Psychology, Utrecht University, The Netherlands
[e] MRC Unit on Anxiety & Stress Disorders, University of Cape Town, South Africa

ARTICLE INFO

Keywords:
Fear
Avoidance
Aggression
Testosterone
Orbitofrontal cortex

ABSTRACT

Recent evidence suggests that the steroid hormone testosterone can decrease the functional coupling between orbitofrontal cortex (OFC) and amygdala. Theoretically this decoupling has been linked to a testosterone-driven increase of goal-directed behaviour in case of threat, but this has never been studied directly. Therefore, we placed twenty-two women in dynamically changing situations of escapable and inescapable threat after a within-subject placebo controlled testosterone administration. Using functional magnetic resonance imaging (fMRI) we provide evidence that testosterone activates the left lateral OFC (LOFC) in preparation of active goal-directed escape and decouples this OFC area from a subcortical threat system including the central-medial amygdala, hypothalamus and periaqueductal gray. This LOFC decoupling was specific to threatening situations, a point that was further emphasized by an absence of such decoupling in a second experiment focused on resting-state connectivity. These results not only confirm that testosterone administration decouples the LOFC from the subcortical threat system, but also show that this is specifically the case in response to acute threat, and ultimately leads to an increase in LOFC activity when the participant prepares a goal-directed action to escape. Together these results for the first time provide a detailed understanding of functional brain alterations induced by testosterone under threat conditions, and corroborate and extend the view that testosterone prepares the brain for goal-directed action in case of threat.

1. Introduction

The steroid hormone testosterone has a well-established role in the reduction of fear and the promotion of dominance motivation and aggression in many species (Mazur and Booth, 1998; Wingfield et al., 1990). In humans, the neural mechanisms underlying these effects are not yet clear, but it has been suggested that testosterone administration can decouple the orbitofrontal cortex (OFC) from subcortical threat reactivity, leading to an increase in impulse-driven and goal-directed behaviour in response to threat (Terburg and van Honk, 2013b; van Honk et al., 2011). Direct evidence for this hypothesis is however currently lacking as acute threat reactivity in the brain and associated goal-directed behaviour have not yet been studied in relation to testosterone administration.

We do know that testosterone can reduce physiological fear responses in humans (Hermans et al., 2007, 2006), and testosterone has repeatedly been linked to subcortical-cortical decoupling (Schutter and van Honk, 2004) and decoupling of the OFC from the amygdala in particular (Bos et al., 2012a; van Wingen et al., 2010; Volman et al., 2011, 2016). Although the specific functions ascribed to the OFC are highly diverse (Stalnaker et al., 2015), it is generally accepted that its coupling with the amygdala serves to adjust behaviour based on the integration of top-down goal-directed action tendencies and bottom-up emotional reactivity (Kringelbach and Rolls, 2004; Milad and Rauch, 2007; Murray and Izquierdo, 2007; Zald et al., 2014). We aimed to tap into this function by means of a functional magnetic resonance imaging (fMRI) experiment with dynamically changing situations of acute threat with goal-directed escape possibilities (Montoya et al., 2015). We applied this experiment in a double-blind placebo-controlled testosterone administration design along with a measurement of baseline resting-state fMRI (RS-fMRI) connectivity. Using this design, we were able to investigate the hypothesis that testosterone's decoupling of the OFC

* Corresponding author at: Utrecht University, Department of Psychology, Heidelberglaan 1, 3584 CS, Utrecht, The Netherlands.
E-mail address: d.terburg@uu.nl (D. Terburg).

https://doi.org/10.1016/j.psyneuen.2018.05.038
Received 24 November 2017; Received in revised form 7 May 2018; Accepted 29 May 2018

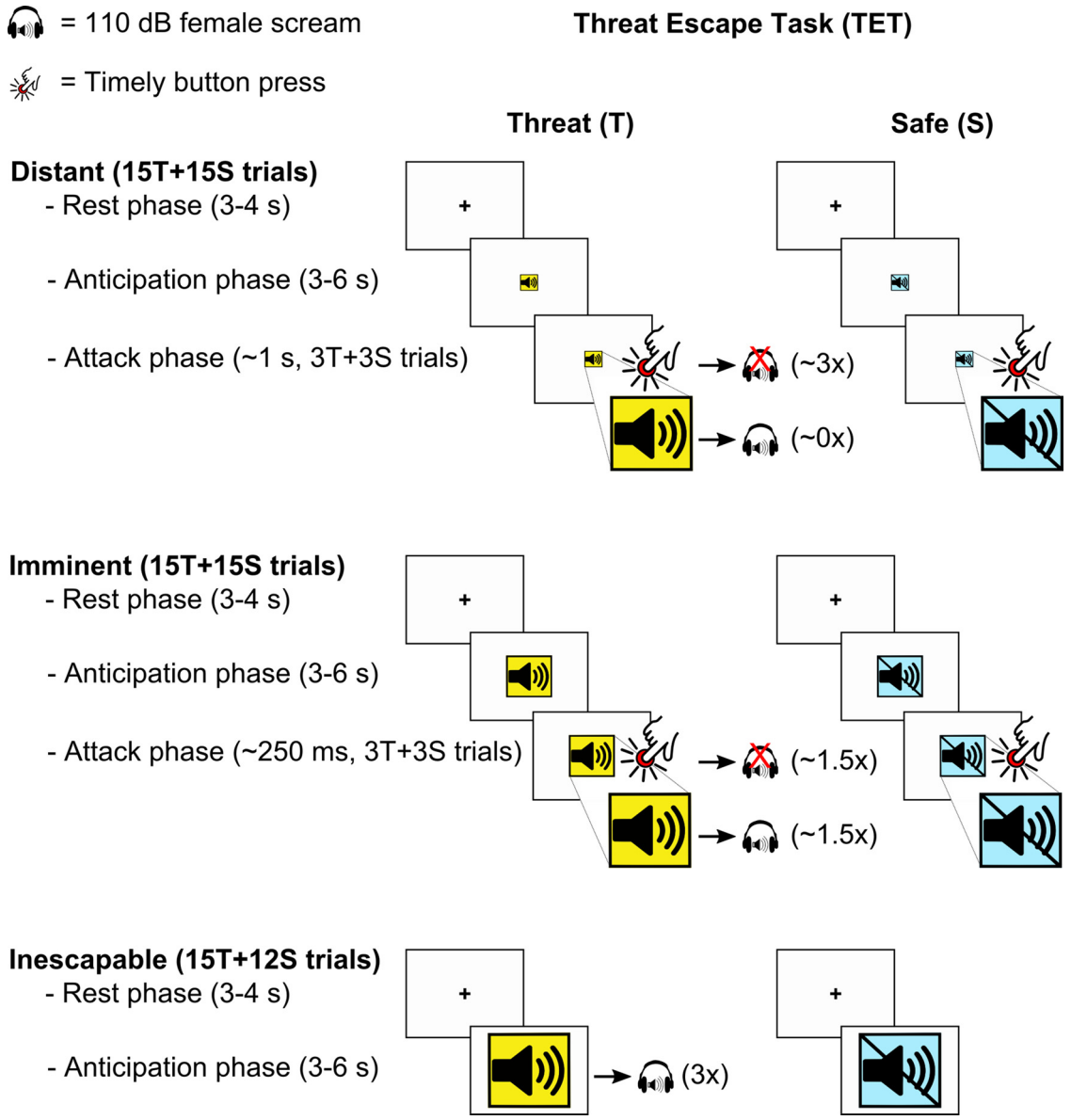

Fig. 1. Outline of the threat escape task. Participants are repeatedly attacked by rapidly approaching pictures. Participants can escape by pressing a button, but when they fail to do so they will be presented with a highly aversive noise (AN). The pictures are manipulated to be distant-escapable, imminent (escapable at chance-level) or inescapable, and all conditions are compared with an equivalent safe-context control condition involving the same procedure but without the threat of AN exposure.

from the amygdala is directly involved in threat and escape anticipation.

2. Methods

2.1. Participants

Thirty healthy young women were recruited to participate in the experiment. Ethical approval was granted by the Human Research Ethics Committee of the University of Cape Town (UCT). Before being invited to participate, all women were screened with self-report questionnaires for present or previous psychiatric conditions. Additional exclusion criteria, also assessed by self-report questionnaire, were: Current or recent use of psychotropic medications, use of hormonal contraceptives, pregnancy, abnormal menstrual cycle, any endocrine disorders, any other serious medical condition, left-handedness, habitual smoking, hearing problems, and colour blindness. Upon their arrival at the laboratory, all participants provided written informed consent before testing began. After recruitment, four participants were unable to complete their scans: One did not fit in the head coil, and three could not complete scans due to electricity failure at the scan facility. This left 26 participants who were included in the resting state analyses. A further four were excluded from the task-based statistical analyses: One due to excessive head movement in the scanner (40 mm) during the task, one due to coil signal failure, and two due to headphone failure. After these 8 exclusions, the total sample consisted of 22 participants (age range 18–37, mean age 21.3, $SD = 4.4$), with 11 in each administration order (placebo in first session, or testosterone in first session). Only women were considered as participants because the parameters (quantity and time course) for inducing neurophysiological effects after a single sublingual administration of 0.5 mg of testosterone are known in women, whereas these parameters are not known in men (Tuiten et al., 2000). Each participant was paid ZAR250 for their participation.

2.2. Drug administration

We followed the procedure first reported by Tuiten et al. (2000), which involves the sublingual administration of 0.5 mg of testosterone with a hydroxypropyl-β-cyclodextrin carrier (manufactured by Laboswiss AG, Davos, Switzerland) to healthy young women. Placebo samples were similar except for the omission of testosterone. This is a well-established single dose testosterone administration procedure that has been widely used for nearly two decades (Tuiten et al., 2000, 2018) and has repeatedly been shown to generate behavioural effects in young women (see Bos et al., 2012b; van Honk et al., 2014 for reviews). For the dosage chosen, no side effects have been reported in this or other studies to date. See supplementary information for a more detailed description of this administration method.

2.3. Procedure/experimental design

Participants were tested on two separate days. The first and second session were separated by at least 48 h. Both testing days fell within the follicular phase of the participants' menstrual cycles to ensure low and stable basal levels of sex hormones (e.g. progesterone, luteinizing hormone, and follicle stimulating hormone). On both occasions, participants arrived at the lab to receive the drug or placebo administration in the morning. Participants were instructed not to participate in any activity that could cause excessive fluctuations in hormone production, such as sports games, exams, or sexual activity. Four hours after administration they returned to the lab to undergo MRI scanning. This experiment was part of a larger study and all participants participated in two other fMRI tasks, not reported in this paper.

2.4. Threat escape task (TET)

We used an active escape paradigm that has been validated in previous pharmaco-fMRI research (Montoya et al., 2015). The task invokes different stages of threat imminence using visual images that approached (increase in size) the subject, culminating in a highly aversive noise (AN; a 1-second ~110 dB female scream), see Fig. 1. The proximity of the threat, from furthest to nearest, can be distant (easily escapable), imminent (with effort escapable at chance level), or inescapable. Each condition has a matched safe condition without AN presentation, which is distinguishable by a different visual stimulus. Each trial is presented for either 3, 4.5, or 6 s, and trials are separated by rest phases of 3 or 4 s. In all conditions, except for the inescapable condition, the participant can avoid AN presentation by pressing a button in time to prevent the image from reaching full-size. The speed of the approaching threat is controlled based on each participant's baseline reaction times as assessed in a practice session, and is updated based on performance during the experiment. Upon failing to escape an imminent attack, the duration of the following attack would be extended by 33 ms, and when an imminent attack was successfully avoided, the attack duration was shortened by 33 ms. This allows for all participants, regardless of general reaction time speed, to escape from the imminent threat at the same probability, i.e. chance-level performance, resulting in a reliable 50% of these trials with actual AN presentation and thus a uniform level of threat across participants. The easily escapable trials were four times the length of the imminent trials. Furthermore, this design allows for comparison of not only safe and threatening conditions, but also between proximity and escapability of threat. Finally, after the participant's scan session they indicated their consciously experienced level of fear in each of the six task conditions on a Likert scale from 1 ("not afraid at all") to 7 ("very afraid").

2.5. Assessment of mood

In both sessions, before scanning, the participants completed the profile of mood states 2nd edition (POMS-II) to assess baseline mood differences due to drug administration. The POMS-II is a 65-item questionnaire that indexes consciously experienced anger, tension/anxiety, depression, vigour, confusion and friendliness, as well as a combined total mood score, using a 5-point Likert scale (Heuchert and McNair, 2012).

2.6. 2D:4D measurement

Following evidence that prenatal testosterone exposure, as indexed by second-to-fourth digit ratio (2D:4D), drives the effect of testosterone on conscious but not reactive behaviour later in life (Terburg and van Honk, 2013b), we also included this metric to our administration study. On one of their testing days, each participant's right hand was scanned on a flatbed scanner, generating images that allow for accurate measurement of the 2D:4D ratio. Digit lengths were measured in Adobe Photoshop CS5 with the ruler tool from medial finger crease to middle of fingertip (Breedlove, 2010).

2.7. fMRI acquisition

All scans were obtained using a 3 Tesla Magnetom Allegra Siemens dedicated head MRI scanner (Siemens Medical Systems GmBH, Erlangen, Germany) with a four-channel phased array head coil, at the Cape Universities Brain Imaging Centre. Whole brain T2* weighted 2D-Echo Planar Imaging (EPI) functional volumes were acquired with 36 ascending axial slices. The following parameters were used: EPI factor = 64, TR/TE: 2s/27ms, flip angle 70°, FOV (anterior-posterior, inferior-superior, left-right): 64*64*36 slices, voxel size: 3.5 x 3.5 x 4mm. Five volumes from start of the task were discarded to allow MR signal to stabilize, and 438 usable functional volumes were acquired. A T1-weighted high resolution structural scan (magnetization-prepared rapid gradient echo; MPRAGE) was obtained once for each participant using the following parameters: TR/TE: 2.53s/6.6ms, flip angle 7°, FOV 256*256*128mm, voxel size: 1 x 1 x 1.33mm, volume acquisition time: 8 min 33s.

To investigate whether the effect of testosterone on OFC coupling is specific to threat processing or context independent, this study also included a resting-state fMRI session. On the same scanner and during the same session a total of 298 functional volumes were obtained using a standard interleaved EPI sequence using a 64*64*29 FOV, a flip angle of 70°, a TR of 1.6 s, a TE of 27 ms, and a voxel size of 3.75 × 3.75 x 5 mm. During this 10-minute scan participants were instructed to remain awake and to try and clear their minds while looking at a fixation cross.

2.8. TET analysis

2.8.1. Preprocessing

MR scans were analysed using SPM8 (Wellcome Department of Imaging Neuroscience, London, UK). Pre-processing included; slice-time correction, motion correction of the 6 motion parameters and the sum of squared difference minimization, volume realignment to the middle volume and AC-PC realignment to improve co-registration. Functional and structural volumes were co-registered and subsequently normalized to Montreal Neurological Institute (MNI) space using unified segmentation procedure (Ashburner and Friston, 2005) and re-sampled into 2 mm isotropic voxels using 4th degree B-spline interpolation. Finally, all images were smoothed using an 8 mm FWHM Gaussian kernel.

2.8.2. Functional activation analysis

The effects of testosterone on brain activity related to threat anticipation were investigated within general linear models (GLM). The task was designed to measure anticipatory BOLD responses to passively experiencing, or actively escaping from, AN exposure. Therefore, trials without actual attacks (12 trials for each condition) were of main

interest, whereas trials with attacks (3 trials for each condition excluding safe/inescapable) were treated as separate variables in the model, which ensures that the effects of motion related artefacts due to button-presses and AN presentation do not affect our measure of interest. Thereto, in the first-level GLM for each test-session, we used twelve regressors for our trials of interest: Six for the trial-onsets (box-car function for stimulus-duration, 3–6 s), and six for the trial-offsets (delta function). Trial-offset regressors were included based on a previous study into threat-offset effects (Klumpers et al., 2010) but considered of no-interest for the current study. Furthermore, ten other nuisance regressors were defined: Five for the trial-onsets for stimuli that would attack, four for the attack-onset (box-car function for attack-duration), and one for the AN-onset (box-car function for AN-duration, 1 s).

These regressors were all convolved with the hemodynamic response function as implemented in the SPM8 software. In addition, realignment parameters and a discrete cosine transform high-pass filter with a 1/128 Hz cut-off frequency were added to the model to reduce variance due to nuisance factors such as movement and drifts in the signal. Thus, in total twenty-nine regressors were entered in the first level statistical analysis. For each subject, and session, we computed contrast maps for onset of distant-escapable, imminent-escapable and inescapable threat and safe cues versus baseline.

For the second level analysis, these contrast maps were entered in a full-factorial 2 × 2 x 3 ANOVA design with drug (testosterone and placebo), condition (threat and safe) and distance (distant-escapable, imminent-escapable, inescapable) as within-subject factors. To evaluate our hypotheses within this GLM we first tested for threat related (de) activations in each distance condition (e.g. Inescapable [Threat < > Safe], etc.). We next tested the two crucial comparisons, which are (de)activations in anticipation of escapable versus inescapable threat (i.e. (Distant[Threat > Safe] + Imminent[Threat > Safe]) / 2 < > Inescapable[Threat > Safe]), and (de)activations in anticipation of high versus low threat (i.e. (Imminent[Threat > Safe] + Inescapable[Threat > Safe]) / 2 < > Distant[Threat > Safe]). Finally, we compared (de)activations between all combinations of distances (e.g. Distant[Threat > Safe] < > Inescapable[Threat > Safe], etc.). This three-step approach was used for general task effects as well as for testosterone administration effects.

For identification of brain (de)activation patterns we first applied whole-brain FWE-correction with a cluster-wise threshold of $p < .05$ and cluster-defining threshold $p < .001$. Next we aimed to identify anatomically specific effects in the OFC and subcortical threat network by applying FWE-correction for the region of interest (ROI) volume with a voxel-wise threshold of $p < .05$. The ROIs consisted of a bilateral midbrain mask based on the TD Lobes atlas from the WFU Pickatlas Toolbox implemented in SPM (Maldjian et al., 2003), a bilateral amygdala mask (Amunts et al., 2005) taken from the anatomy toolbox as implemented in SPM8 (Eickhoff et al., 2005), a bilateral hypothalamus mask created by defining an 8mm sphere around the central coordinate (MNI coordinate: x = 0, y = 2, z = 13) of hypothalamus sub-regions as described by Baroncini et al (2012); (see also Terburg et al., 2013a), and a bilateral OFC mask which includes the areas that were sensitive to testosterone decoupling in previous studies (Bos et al., 2012a; van Wingen et al., 2010; Volman et al., 2011, 2016), namely the rectus and orbital parts of the superior, medial and middle frontal gyri as defined in the AAL template (Tzourio-Mazoyer et al., 2002). See Fig. 2 for a visualisation of these ROIs. Whole brain task effects were linked to anatomical location using the AAL template.

2.8.3. Functional connectivity analysis

Psycho-Physiological interaction (PPI) analysis (Friston et al., 1997) was performed to determine the functional connectivity of the OFC with other brain regions using the PPI module implemented in SPM8. In short, a volume of interest (VOI) was created using a 6 mm sphere around the peak-voxel coordinate of OFC activation identified in the functional activation analysis. For each participant time-course (first-eigenvariate) was extracted, and mean-corrected for general task effects. A new GLM was obtained using this time-course as regressor together with a regressor for the task-contrast of interest, and their interaction (i.e. PPI). To maintain power, we limited this analysis to the identification of connectivity differences in the overall condition contrast (threat versus safe). Finally, contrast-maps of the PPI were entered in separate full-factorial models to test for testosterone administration effects on threat-related OFC connectivity. Although this approach does not allow testing for connectivity modulations based on specific threat distances, it does provide insight into connectivity pattern modulations across dynamically changing threatening compared to safe conditions in general.

2.9. RS-fMRI analysis

2.9.1. Preprocessing

Functional and anatomical images were processed using the fMRI Signal Processing Toolbox for MATLAB (Patel et al., 2014). Anatomical images were skull-stripped. Functional image pre-processing consisted of core image processing and denoising. Core image processing started with slice timing correction with the middle slide as the reference. All frequencies except Nyquist and zero frequencies were kept. Rigid-body parameters (3 rotations and 3 translations) and their first derivatives necessary for head movement correction were calculated and all functional images were aligned to the first frame. Next, affine transformations were calculated and used to co-register the functional data to the skull-stripped anatomical image using a grey matter mask. Zeropadding temporarily added 100 zeros to the end of the time series to prevent errors in denoising the data at a later stage. The data were then transformed to the Montreal Neurological Institute template (average of 152 brains; MNI152), T1 weighted, in standard space by non-linear warping. Generating the CSF/WM signal involved segmentation of the downsampled anatomical dataset to obtain CSF and WM signals from the MNI152 template included in the signal processing toolbox.

Head movement during fMRI scans have been shown to affect functional connectivity measures such as decreased long-distance correlations and increased short-distance correlations (Van Dijk et al., 2012). Traditional methods can remove some artefacts, but are not able to correct for subtler artefacts, such as spike-like movements that lead to spin-history effects. We used a data-driven method that identifies, models, and removes motion artefacts by wavelet despiking (Patel et al., 2014), without the need for data scrubbing. This method first decomposes the time series into a set of scales using the Maximal Overlap Discrete Wavelet Transform (MODWT). It then identifies maximal and minimal wavelet coefficients and detects and removes chains of these coefficients. Such chains are present across multiple scales at the same point in time and represent transients of all sizes. Lastly, the time series are recomposed from the remaining coefficients using inverse MODWT (iMODWT). After wavelet despiking, motion, motion derivatives, CSF and white matter were regressed out.

2.9.2. Seed-based connectivity analysis

To assess OFC connectivity modulations by testosterone, the pre-processed wavelet despiked images were band-pass filtered (0.1–0.01 Hz) and average time-series were extracted for the same OFC sphere used in the PPI analyses of the TET. Whole-brain connectivity maps were calculated based on Pearson correlations between the seed time series and the rest of the brain. The resulting connectivity maps were *z*-transformed, and these were analysed in SPM8 using a pairwise comparison and the same statistical thresholds as used in the TET analyses. To further explore connectivity modulations by testosterone, we also performed this analysis using the three, bilateral, amygdala sub-nuclei seeds obtained from an anatomical connectivity derived amygdala sub parcellation (Bzdok et al., 2013).

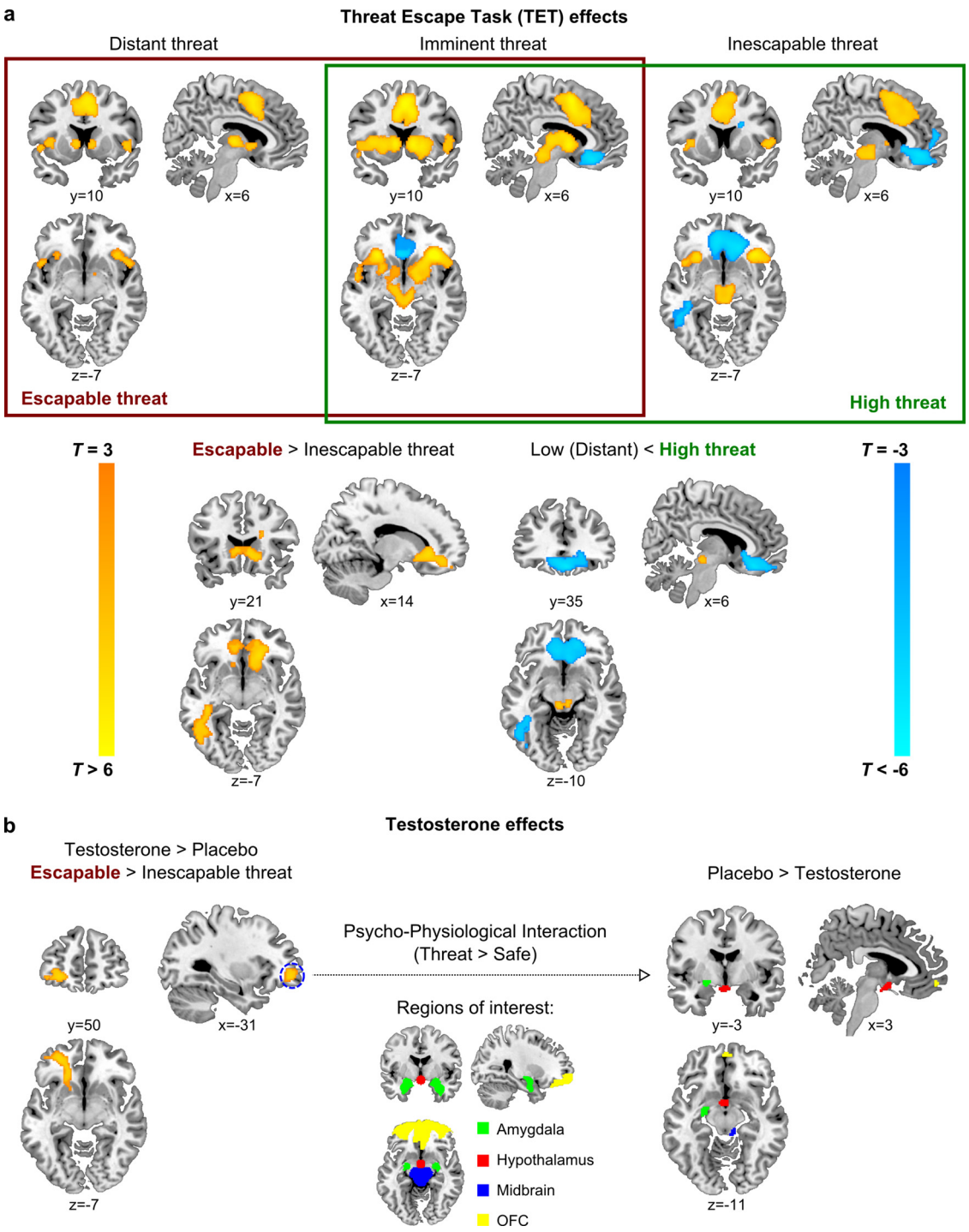

Fig. 2. Functional MRI findings, only significant clusters are shown. a, TET effects: All three threat conditions reliably activated the brain's salience network consisting of the anterior insula, dorsal ACC, thalamus and striatum. The medial prefrontal cortex deactivated particularly when under high threat conditions, the midbrain particularly reacted to high threat, and threat evoked increased striatal activity particularly when it was escapable. b, Testosterone effects: Testosterone activated the left lateral OFC in response to escapable threat, and decoupled this OFC cluster from the midbrain (PAG), left amygdala (CMA), hypothalamus and medial OFC in threat compared to safe conditions.

2.9.3. Whole-brain connectivity analysis

In addition to the hypothesis driven seed-based resting-state connectivity analysis, we also employed a data-driven independent component analysis (ICA) to explore potential whole brain effects of testosterone on functional connectivity. Seed-based analyses only focus on very specific networks and connections. In contrast, independent component analysis makes no assumptions about the underlying networks and thus allows a model-free analysis of any potential differences. Analyses were carried out using Probabilistic Independent Component Analysis (Beckmann and Smith, 2004) as implemented in MELODIC (Multivariate Exploratory Linear Decomposition into Independent Components) Version 3.14, part of FSL (FMRIB's Software Library, www.fmrib.ox.ac.uk/fsl). The following steps were applied to the pre-processed wavelet despiked data: masking of non-brain voxels; voxel-wise de-meaning of the data; normalisation of the voxel-wise variance. Pre-processed data were whitened and projected into a 35-

dimensional subspace using probabilistic Principal Component Analysis where the number of dimensions was estimated using the Laplace approximation to the Bayesian evidence of the model order (Beckmann and Smith, 2004), thus resulting in 35 independent components. The whitened observations were decomposed into sets of vectors which describe signal variation across the temporal domain (time-courses), the session/subject domain and across the spatial domain (maps) by optimising for non-Gaussian spatial source distributions using a fixed-point iteration technique (Hyvarinen, 1999). Estimated Component maps were divided by the standard deviation of the residual noise and thresholded by fitting a mixture model to the histogram of intensity values (Beckmann and Smith, 2004). Permutation testing was used to assess potential effects of testosterone across all 35 components, using 5000 permutations and a threshold free cluster enhancement (TFCE) to control for multiple comparison as implemented in FSL's randomise tool (Winkler et al., 2014).

2.10. Data availability

Non-thresholded statistical maps of the main fMRI analyses can be found at the NeuroVault data repository (Gorgolewski et al., 2015): http://neurovault.org/collections/AUIXVATH/ and http://neurovault.org/collections/ISHJRKRU/. All other data are available on request from the authors.

3. Results

3.1. Subjective experience data

Participants were asked to guess which session had included the testosterone dose and they were unable to correctly guess above chance ($\chi 2 = 0.2338$, $p = 0.63$). Additionally, POMS-II mood scales showed no difference on the total mood scale (Heuchert and McNair, 2012) between drug conditions ($t(22) = 0.928$, $p = 0.364$), and when looking at the separate moods this was also the case for anger, vigour, confusion, tension, and fatigue (all $ps > 0.38$). Depression was significantly lower in the testosterone (1.07, $SD = 0.12$) compared to placebo (1.15, $SD = 0.20$) condition ($t(21) = 2.791$, $p = 0.011$), but this small difference could be considered negligible as in both conditions these scores are near the absolute minimum of score '1' which in the 5-point Likert scale represents 'no depression at all'.

The fear ratings regarding the AN, rated on a 7-point Likert scale, were generally high in both drug conditions (testosterone: $M = 5.71$, $SD = 1.34$; placebo: $M = 6.12$, $SD = 1.01$) and over both sessions (session 1: $M = 6.02$, $SD = 1.02$; session 2: $M = 5.82$ $SD = 1.36$). Across both drug conditions, participants reported greater fear in the threat vs safe condition (t(21) = -21.39, p < 0.001) and also in the inescapable vs imminent (t(21) = -3.65,p < 0.001), and imminent vs avoidable conditions (t(21) = 4.68, p < 0.001). Paired sample *T*-tests confirmed no significant difference between the two drug conditions ($t(21) = -1.7$, $p = 0.103$) or between the two sessions ($t(21) = -0.78$, $p = 0.444$).

3.2. TET results

3.2.1. General task effects

Statistics and results for the TET are summarized in Table 1, Fig. 2, and see http://neurovault.org/collections/AUIXVATH/ for non-thresholded statistical maps. In line with previous work on acute and escapable threat (Klumpers et al., 2010; Mobbs et al., 2007; Montoya et al., 2015), we observed reliable threat-potentiated activity in the salience network of the brain (anterior insula, dorsal anterior cingulate cortex, thalamus, bed nucleus of the stria terminalis and striatum) in all three distance conditions. Furthermore, both high threat conditions (imminent and inescapable) evoked midbrain activity, and both escapable threat conditions (distant and imminent) evoked hypothalamic reactions. Threat-related deactivations were observed in the medial prefrontal cortex, including the medial OFC (MOFC), particularly in the high threat conditions, and inescapable threat also deactivated areas in the medial temporal cortex and the angular gyrus.

As can be seen in Table 1 and Fig. 2, analysis of threat level and escapability revealed that high threat evoked midbrain reactivity, corresponding to the location of the periaqueductal gray (see Hermans et al., 2013), and deactivations in medial prefrontal cortex. Striatal reactivity to threat was strongest when the threat was escapable. Thus, in line with previous studies (Klumpers et al., 2010; Mobbs et al., 2007; Montoya et al., 2015) an approaching threat shifts brain activity away from cortical towards subcortical processing, with anticipation of an active escape response evoking striatal threat reactivity.

3.2.2. Testosterone administration effects

Testosterone had no direct effect on threat reactivity in the three distance conditions separately[1], but did increase activity in the left lateral OFC (LOFC) in escapable compared to inescapable threatening conditions (see Fig. 2). Post-hoc *T*-tests showed this was due to an increase to escapable rather than a decrease to inescapable threat (see Table 1).

PPI-analysis (see methods) using the location of this LOFC cluster revealed that testosterone administration reduced threat-related connectivity with the midbrain, hypothalamus, left amygdala and MOFC (see Fig. 2). More specific allocation of the midbrain cluster indicated that it corresponds to the location of the periaqueductal gray (see Hermans et al., 2013), and the amygdala cluster corresponds to the left central-medial amygdala (CMA; see Amunts et al., 2005). Finally, post-hoc *T*-tests revealed that specifically in the testosterone condition left-sided LOFC-CMA coupling was reduced in threat compared to safe conditions.

3.2.3. 2D:4D analysis

To investigate the relation between testosterone administration effects and 2D:4D, beta weights were extracted from a 6 mm sphere around the LOFC peak activation identified in the testosterone/TET analysis. These beta-weights were entered in a 2 (testosterone and placebo) x 2 (threat and safe) x 3 (distant, imminent, and inescapable) repeated measures ANOVA with 2D:4D as covariate. The 2D:4D covariate was non-significant ($F(1,20) = 0.443$, $p = .513$), which was also the case for its interactions with the within-subjects variables (all $ps > .16$).

3.3. RS-fMRI results

To specifically investigate testosterone's effect during resting state, whole-brain correlation maps (based on Fischer *z*-transformed Pearson correlation maps) were computed for the LOFC seed. In both drug conditions left LOFC connectivity was particularly strong with the right OFC, bilateral striatum and anterior cingulate cortex (see Fig. 3). Pairwise comparisons indicated no significant differences between placebo and testosterone, even when applying a more liberal threshold ($p < .01$ as cluster-defining threshold). Confidence interval plots for the pairwise comparisons are available in the supplementary material. Similarly, pairwise comparisons of the *z*-maps also indicated no significant differences between placebo and testosterone for any of the amygdala seeds (Bzdok et al., 2013) using the same liberal thresholds, and exploratory ICA analysis did not reveal any differences between drug conditions (see http://neurovault.org/collections/AUIXVATH/ for seed-based non-thresholded statistical maps and http://neurovault.org/collections/ISHJRKRU/ for the 35 identified ICA components).

[1] This was also the case when applying a more liberal threshold; $p < .01$ as cluster-defining threshold.

Table 1
Functional MRI findings from the TET. All reported clusters are activations (or deactivations, indicated with a negative *T*-value) to threat > safe contrasts. Clusters are whole-brain statistics FWE cluster-wise corrected ($p < .05$) with cluster defining threshold $p < .001$, or in case of region of interest analysis (indicated with *, and see Fig. 2 for a visualisation) FWE voxel-wise corrected ($p < .05$). PFC = Prefrontal Cortex, OFC = Orbitofrontal Cortex, BNST = Bed Nucleus of the Stria Terminalis, s.c. = same cluster.

Structure	Hemisphere	Cluster size	*p*-value	Peak *T*-value	MNI-coordinate		
					X	Y	Z
Threat effects							
Inescapable							
Anterior Insula	Left	571	0.006	5.43	−32	20	4
	Right	793	0.001	5.67	34	24	−6
Anterior Cingulate Cortex	Both	1986	< .001	4.8	−6	10	38
Supplemental Motor Area	Both	s.c.					
Striatum	Both	872	0.001	4.45	−10	4	0
Thalamus	Both	s.c.					
Midbrain	Both	s.c.					
BNST	Both	s.c.					
Midbrain*	Both	321	0.002	4.39	8	−14	−10
Angular Gyrus	Left	480	0.012	−4.65	−48	−60	28
	Right	508	0.01	−4.61	50	−66	32
Medial OFC	Both	3049	< .001	−4.89	−8	40	−8
Medial Temporal Cortex	Left	617	0.004	−4.69	−48	−38	0
Medial OFC*	Both	551	< .001	−4.89	−8	40	−8
Imminent							
Anterior Insula	Both	6554	< .001	7.23	32	26	−4
Striatum	Both	s.c.					
Thalamus	Both	s.c.					
Midbrain	Both	s.c.					
BNST	Both	s.c.					
Anterior Cingulate Cortex	Both	2245	< .001	6.03	2	10	48
Supplemental Motor Area	Both	s.c.					
Hypothalamus*	Both	5	0.041	2.91	−2	−2	−6
Midbrain*	Both	372	< .001	4.44	6	−26	−10
Medial OFC	Both	682	0.002	−4.99	4	30	-14
Dorsomedial PFC	Left	441	0.017	−4.87	−20	32	44
Medial OFC*	Both	227	< .001	−4.99	4	30	−14
Distant							
Anterior Insula	Left	897	< .001	5.55	−36	20	4
	Right	706	0.002	5.97	36	24	4
Anterior Cingulate Cortex	Both	1612	< .001	6.53	−6	4	48
Supplemental Motor Area	Both	s.c.					
Striatum	Both	879	0.001	5.07	8	−12	4
Thalamus	Both	s.c.					
BNST	Both	s.c.					
Hypothalamus*	Left	31	0.013	3.28	−6	−4	−12
Threat escapability effects							
Escapable > Inescapable							
Medial PFC	Both	1831	< .001	4.65	18	30	−4
Striatum	Both	s.c.					
Medial Temporal Cortex	Left	763	0.001	4.18	−42	−40	0
Medial OFC*	Left	11	0.017	4.1	−6	56	−18
High > Low							
Midbrain*	Left	10	0.02	3.75	−6	−26	−10
Medial OFC	Both	1607	< .001	−5.11	2	34	−16
Dorsomedial PFC	Left	367	0.033	−4.39	−14	60	18
Medial Temporal Cortex	Left	465	0.014	−4.01	−52	−56	−8
Medial OFC*	Both	373	< .001	−5.11	2	34	−16
	Left	40	0.007	−4.35	−10	52	−16
Distant > Imminent							
Medial OFC*	Both	90	0.003	4.56	4	30	−14
Imminent > Inescapable							
Striatum	Both	635	0.003	4.24	18	28	−4
Distant > Inescapable							
Medial PFC	Both	2260	< .001	4.75	10	24	−4
Striatum	Both	s.c.					
Medial Temporal Cortex	Left	1062	< .001	4.25	−40	−32	−6
Medial OFC*	Both	367	0.004	4.48	−6	56	−18
Drug, threat escapability interactions							
Testosterone > Placebo: Escapable > Inescapable							
Lateral OFC	Left	347	0.04	4.39	−28	48	−6
Striatum	Left	s.c.					
Lateral OFC*	Left	27	0.006	4.39	−28	48	−6
Testosterone > Placebo: Escapable							
Lateral OFC*	Left	2	0.044	3.82	−28	50	−4
Testosterone > Placebo: Distant > Inescapable							
Lateral OFC*	Left	19	0.006	4.39	−28	48	−6

(*continued on next page*)

Table 1 (*continued*)

Structure	Hemisphere	Cluster size	*p*-value	Peak *T*-value	MNI-coordinate		
					X	Y	Z
Drug, psycho-physiological interactions							
PPI of Threat > Safe with LOFC signal: Placebo > Testosterone							
Medial Temporal Cortex	Right	1539	< .001	5.44	60	−44	14
Superior Temporal Cortex	Right	785	< .001	5.33	54	−22	2
Anterior Insula	Right	s.c.					
Striatum	Right	s.c.					
Hypothalamus*	Both	67	0.012	3.58	0	−4	−18
Midbrain*	Right	13	0.018	4.14	10	−32	−12
Medial OFC*	Both	12	0.024	4.44	2	56	−10
Amygdala*	Left	45	< .001	5.33	−22	−8	−8
PPI of Threat > Safe with LOFC signal: Testosterone							
Amygdala*	Left	26	0.003	−4.64	−26	−8	−8

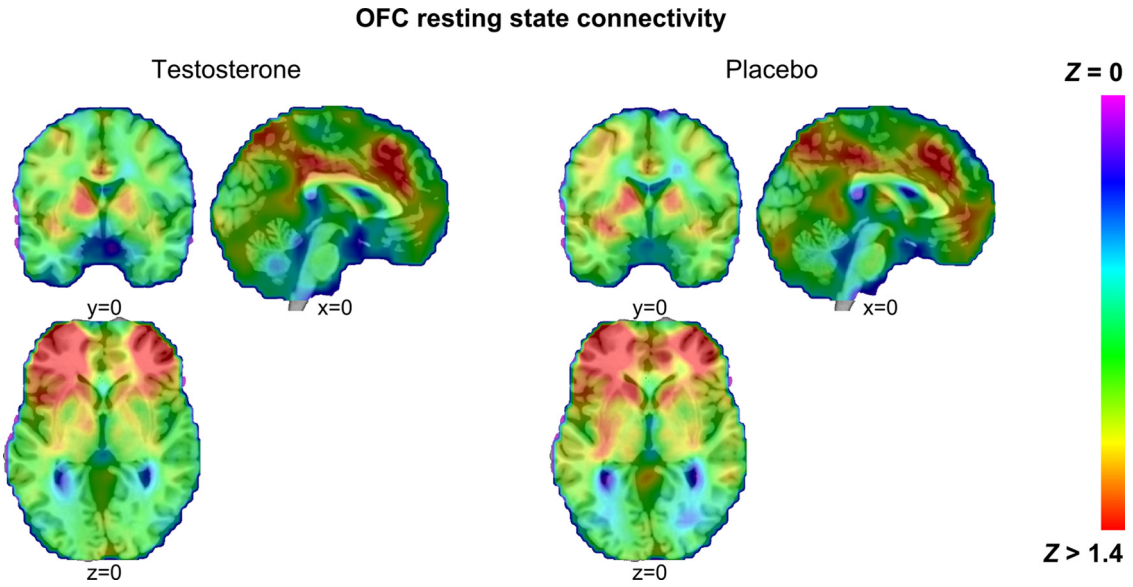

Fig. 3. Resting state connectivity of the left lateral OFC. Connectivity was particularly strong with the bilateral OFC, striatum and anterior cingulate cortex. This pattern was similar after testosterone and placebo administration.

4. Discussion

This study provides evidence that a single administration of testosterone changes the activation and connectivity pattern of the left LOFC particularly in response to acute threat. Testosterone activates the left LOFC in situations of goal-directed escape anticipation, and decouples the left LOFC from a subcortical threat network (i.e. CMA, hypothalamus, and PAG) during threatening compared to safe situations.

To start with the latter, this testosterone induced LOFC-subcortex decoupling can theoretically either constitute a loss of top-down control over the subcortical threat system, or a decrease of bottom-up input to the LOFC. We cannot assess the direction of this effect directly in the present data, but given that we find reliable threat-reactivity in this subcortical threat system, which does not change after testosterone administration, a loss of top-down control seems unlikely. Alternatively, testosterone might act to prevent subcortically generated threat reactivity from influencing the OFC. Following the view that OFC-amygdala connectivity serves to adjust behaviour based on the integration of top-down goal-directed action tendencies and bottom-up affective reactivity (Kringelbach and Rolls, 2004; Milad and Rauch, 2007 Murray and Izquierdo, 2007 Zald et al., 2014), testosterone might therefore push OFC processing towards goal-directed action. Further support for this view can be found in our observation that testosterone specifically boosts LOFC activity in situations that require such a goal-directed action, i.e. active escape from a threat. Although we cannot assess any behavioural benefit from this testosterone-driven LOFC activity with the present design –given that it adjusts to the behaviour of the participant to keep threat levels stable across participants– these results do follow the hypothesis that testosterone can promote goal-directed action in case of threat (Terburg and van Honk, 2013b; van Honk et al., 2011).

An interesting aspect of the present findings is the functional distinction between LOFC and MOFC. Both areas are structurally (Murray and Izquierdo, 2007) and functionally (Zald et al., 2014) connected to the amygdala, but in the MOFC this connection has been linked to impulse control and reward drive, whereas in the LOFC it has been linked to adjustment of behaviour in case of potential punishment (Kringelbach and Rolls, 2004; Milad and Rauch, 2007). This seems to be in line with the MOFC deactivation in response to high threat observed here and in previous studies (Mobbs et al., 2007; Montoya et al., 2015). Moreover, the fact that testosterone boosts the LOFC particularly in situations of goal-directed escape anticipation seamlessly links to the LOFC's sensitivity to potentially punishing or dangerous situations.

Interestingly, testosterone has also been linked to a down regulation of MOFC activity in relation to social aggression (Mehta and Beer, 2010). The possibility that this reflects reduced impulse control is consistent with evidence that testosterone levels in adolescent boys predict reduced MOFC-amygdala connectivity and increased alcohol use (Peters et al., 2015). Furthermore, increased socially aggressive

impulses have been observed in a range of testosterone administration studies (e.g. Terburg et al., 2012, 2016; van Honk et al., 2001), and have been associated with activation in the subcortical threat system (Goetz et al., 2014; Hermans et al., 2008).

A possible confound in a threat-escape task is that individual differences in performance can potentially affect likelihood of receiving the aversive stimulus. We controlled for this possibility by adjusting the attack-speed of the task-stimuli to the individual performance such that the imminent conditions were escapable in ~50% of the cases for each individual. This adjustment created a situation wherein distant threats were always, and for each and every participant, easily escapable, imminent threats were always very hard to escape from (~50%) and inescapable threats were always inescapable. This was done in order to ensure that threat-type and escapability are exactly similar for all our participants, but introduces the limitation that escape performance cannot be directly measured. Our results should therefore be interpreted in relation to the preset escapability levels (i.e. distant, imminent and inescapable) and not in terms of individual escape performance.

Taken together, these data provide a solid foundation for the view that testosterone decouples the OFC from the amygdala under threat (Terburg and van Honk, 2013b; van Honk et al., 2011). In this framework, the here observed reduction of bottom-up amygdala-LOFC coupling serves goal-directed action, while reductions in top-down control from the MOFC underlie risk taking and social aggression. Future studies should address this interplay of testosterone with fear and aggression directly, with the hypothesis that testosterone prepares the human brain for aggressive as well as evasive action in response to threat by decoupling the OFC from the subcortical threat system.

Conflict of interest

DJS is supported by the Medical Research Council of South Africa and has received research grants and/or consultancy honoraria from: Abbott, Astrazeneca, Eli-Lilly, GlaxoSmithKline, Jazz Pharmaceuticals, Johnson & Johnson, Lundbeck, Orion, Pfizer, Pharmacia, Roche, Servier, Solvay, Sumitomo, Takeda, Tikvah, and Wyeth. The other authors declare no conflict of interest.

Acknowledgements

The material presented in this study is original research, has not been previously published and has not been submitted for publication elsewhere. This work was supported by the South African National Research Foundation (NRF), and the University of Cape Town (Brain Behaviour Unit). The funding sources had no role in study design, data collection, analysis and interpretation, nor in writing of this report. DT (VENI 451-13-004), JvH (Brain and Cognition 056-24-010), and PAB (VENI 451-14-015) were supported by the Netherlands Society of Scientific Research.

Appendix A. Supplementary data

Supplementary material related to this article can be found, in the online version, at doi:https://doi.org/10.1016/j.psyneuen.2018.05.038.

References

Amunts, K., Kedo, O., Kindler, M., Pieperhoff, P., Mohlberg, H., Shah, N.J., Habel, U., Schneider, F., Zilles, K., 2005. Cytoarchitectonic mapping of the human amygdala, hippocampal region and entorhinal cortex: intersubject variability and probability maps. Anat. Embryol. (Berl) 210 (5-6), 343–352.
Ashburner, J., Friston, K.J., 2005. Unified segmentation. Neuroimage 26 (3), 839–851.
Baroncini, M., Jissendi, P., Balland, E., Besson, P., Pruvo, J.-P., Francke, J.-P., Dewailly, D., Blond, S., Prevot, V., 2012. MRI atlas of the human hypothalamus. Neuroimage 59 (1), 168–180.
Beckmann, C.F., Smith, S.M., 2004. Probabilistic independent component analysis for functional magnetic resonance imaging. IEEE Trans. Med. Imaging 23 (2), 137–152.
Bos, P.A., Hermans, E.J., Ramsey, N.F., van Honk, J., 2012a. The neural mechanisms by which testosterone acts on interpersonal trust. Neuroimage 61 (3), 730–737.
Bos, P.A., Panksepp, J., Bluthé, R.M., van Honk, J., 2012b. Acute effects of steroid hormones and neuropeptides on human social-emotional behavior: a review of single administration studies. Front. Neuroendocrinol. 33 (1), 17–35.
Breedlove, S.M., 2010. Minireview: organizational hypothesis: instances of the fingerpost. Endocrinology 151 (9), 4116–4122.
Bzdok, D., Laird, A.R., Zilles, K., Fox, P.T., Eickhoff, S.B., 2013. An investigation of the structural, connectional, and functional subspecialization in the human amygdala. Hum. Brain Mapp. 34 (12), 3247–3266.
Eickhoff, S.B., Stephan, K.E., Mohlberg, H., Grefkes, C., Fink, G.R., Amunts, K., Zilles, K., 2005. A new SPM toolbox for combining probabilistic cytoarchitectonic maps and functional imaging data. Neuroimage 25 (4), 1325–1335.
Friston, K.J., Buechel, C., Fink, G.R., Morris, J., Rolls, E., Dolan, R.J., 1997. Psychophysiological and modulatory interactions in neuroimaging. Neuroimage 6 (3), 218–229.
Goetz, S.M., Tang, L., Thomason, M.E., Diamond, M.P., Hariri, A.R., Carre, J.M., 2014. Testosterone rapidly increases neural reactivity to threat in healthy men: a novel two-step pharmacological challenge paradigm. Biol. Psychiatry 76 (4), 324–331.
Gorgolewski, K.J., Varoquaux, G., Rivera, G., Schwarz, Y., Ghosh, S.S., Maumet, C., Sochat, V.V., Nichols, T.E., Poldrack, R.A., Poline, J.B., Yarkoni, T., 2015. NeuroVault.org: a web-based repository for collecting and sharing unthresholded statistical maps of the human brain. Front. Neuroinf. 9, 8.
Hermans, E.J., Putman, P., Baas, J.M., Koppeschaar, H.P., van Honk, J., 2006. A single administration of testosterone reduces fear-potentiated startle in humans. Biol. Psychiatry 59 (9), 872–874.
Hermans, E.J., Putman, P., Baas, J.M., Gecks, N.M., Kenemans, J.L., van Honk, J., 2007. Exogenous testosterone attenuates the integrated central stress response in healthy young women. Psychoneuroendocrinology 32 (8–10), 1052–1061.
Hermans, E.J., Ramsey, N.F., van Honk, J., 2008. Exogenous testosterone enhances responsiveness to social threat in the neural circuitry of social aggression in humans. Biol. Psychiatry 63 (3), 263–270.
Hermans, E.J., Henckens, M.J., Roelofs, K., Fernandez, G., 2013. Fear bradycardia and activation of the human periaqueductal grey. Neuroimage 66, 278–287.
Heuchert, J.P., McNair, D.M., 2012. POMS 2: Profile of Mood States, 2nd edition. .
Hyvarinen, A., 1999. Fast and robust fixed-point algorithms for independent component analysis. IEEE Trans. Neural Netw. 10 (3), 626–634.
Klumpers, F., Raemaekers, M.A., Ruigrok, A.N., Hermans, E.J., Kenemans, J.L., Baas, J.M., 2010. Prefrontal mechanisms of fear reduction after threat offset. Biol. Psychiatry 68 (11), 1031–1038.
Kringelbach, M.L., Rolls, E.T., 2004. The functional neuroanatomy of the human orbitofrontal cortex: evidence from neuroimaging and neuropsychology. Prog. Neurobiol. 72 (5), 341–372.
Maldjian, J.A., Laurienti, P.J., Kraft, R.A., Burdette, J.H., 2003. An automated method for neuroanatomic and cytoarchitectonic atlas-based interrogation of fMRI data sets. Neuroimage 19 (3), 1233–1239.
Mazur, A., Booth, A., 1998. Testosterone and dominance in men. Behav. Brain Sci. 21 (3), 353–363 discussion 363-397.
Mehta, P.H., Beer, J., 2010. Neural mechanisms of the testosterone-aggression relation: the role of orbitofrontal cortex. J. Cogn. Neurosci. 22 (10), 2357–2368.
Milad, M.R., Rauch, S.L., 2007. The role of the orbitofrontal cortex in anxiety disorders. Ann. N. Y. Acad. Sci. 1121, 546–561.
Mobbs, D., Petrovic, P., Marchant, J.L., Hassabis, D., Weiskopf, N., Seymour, B., Dolan, R.J., Frith, C.D., 2007. When fear is near: threat imminence elicits prefrontal-periaqueductal gray shifts in humans. Science 317 (5841), 1079–1083.
Montoya, E.R., van Honk, J., Bos, P.A., Terburg, D., 2015. Dissociated neural effects of cortisol depending on threat escapability. Hum. Brain Mapp. 36 (11), 4304–4316.
Murray, E.A., Izquierdo, A., 2007. Orbitofrontal cortex and amygdala contributions to affect and action in primates. Ann. N. Y. Acad. Sci. 1121, 273–296.
Patel, A.X., Kundu, P., Rubinov, M., Jones, P.S., Vertes, P.E., Ersche, K.D., Suckling, J., Bullmore, E.T., 2014. A wavelet method for modeling and despiking motion artifacts from resting-state fMRI time series. Neuroimage 95, 287–304.
Peters, S., Jolles, D.J., Van Duijvenvoorde, A.C., Crone, E.A., Peper, J.S., 2015. The link between testosterone and amygdala-orbitofrontal cortex connectivity in adolescent alcohol use. Psychoneuroendocrinology 53, 117–126.
Schutter, D.J., van Honk, J., 2004. Decoupling of midfrontal delta-beta oscillations after testosterone administration. Int. J. Psychophysiol. 53 (1), 71–73.
Stalnaker, T.A., Cooch, N.K., Schoenbaum, G., 2015. What the orbitofrontal cortex does not do. Nat. Neurosci. 18 (5), 620–627.
Terburg, D., van Honk, J., 2013b. Approach–avoidance versus dominance–submissiveness: a multilevel neural framework on how testosterone promotes social status. Emot. Rev. 5 (3), 296–302.
Terburg, D., Aarts, H., van Honk, J., 2012. Testosterone affects gaze-aversion from angry faces outside of conscious awareness. Psychol. Sci. 23 (5), 459–463.
Terburg, D., Syal, S., Rosenberger, L.A., Heany, S., Phillips, N., Gericke, N., Stein, D.J., Van Honk, J., 2013a. Acute effects of Sceletium tortuosum (Zembrin), a dual 5-HT reuptake and PDE4 inhibitor, in the human amygdala and its connection to the hypothalamus. Neuropsychopharmacology 38 (13), 2708–2716.
Terburg, D., Syal, S., Rosenberger, L.A., Heany, S.J., Stein, D.J., van Honk, J., 2016. Testosterone abolishes implicit subordination in social anxiety. Psychoneuroendocrinology 72, 205–211.
Tuiten, A., Van Honk, J., Koppeschaar, H., Bernaards, C., Thijssen, J., Verbaten, R., 2000. Time course of effects of testosterone administration on sexual arousal in women. Arch. Gen. Psychiatry 57 (2), 149–153 discussion 155-146.
Tuiten, A., van Rooij, K., Bloemers, J., Eisenegger, C., van Honk, J., Kessels, R., et al., 2018. Efficacy and safety of on-demand use of 2 treatments designed for different

etiologies of female sexual interest/arousal disorder: 3 randomized clinical trials. J. Sex. Med. 15 (2), 201–216.
Tzourio-Mazoyer, N., Landeau, B., Papathanassiou, D., Crivello, F., Etard, O., Delcroix, N., Mazoyer, B., Joliot, M., 2002. Automated anatomical labeling of activations in SPM using a macroscopic anatomical parcellation of the MNI MRI single-subject brain. Neuroimage 15 (1), 273–289.
Van Dijk, K.R., Sabuncu, M.R., Buckner, R.L., 2012. The influence of head motion on intrinsic functional connectivity MRI. Neuroimage 59 (1), 431–438.
van Honk, J., Tuiten, A., Hermans, E., Putman, P., Koppeschaar, H., Thijssen, J., Verbaten, R., van Doornen, L., 2001. A single administration of testosterone induces cardiac accelerative responses to angry faces in healthy young women. Behav. Neurosci. 115 (1), 238–242.
van Honk, J., Terburg, D., Bos, P.A., 2011. Further notes on testosterone as a social hormone. Trends Cogn. Sci. 15 (7), 291–292.
van Honk, J., Bos, P.A., Terburg, D., 2014. Testosterone and dominance in humans: behavioral and brain mechanisms. New Front. Soc. Neurosci. 201–214.
van Wingen, G., Mattern, C., Verkes, R.J., Buitelaar, J., Fernandez, G., 2010. Testosterone reduces amygdala-orbitofrontal cortex coupling. Psychoneuroendocrinology 35 (1), 105–113.
Volman, I., Toni, I., Verhagen, L., Roelofs, K., 2011. Endogenous testosterone modulates prefrontal-amygdala connectivity during social emotional behavior. Cereb. Cortex 21 (10), 2282–2290.
Volman, I., von Borries, A.K., Bulten, B.H., Verkes, R.J., Toni, I., Roelofs, K., 2016. Testosterone modulates altered prefrontal control of emotional actions in psychopathic offenders(1,2,3). eNeuro 3 (1).
Wingfield, J.C., Hegner, R.E., Dufty Jr, A.M., Ball, G.F., 1990. The "challenge hypothesis": theoretical implications for patterns of testosterone secretion, mating systems, and breeding strategies. Am. Naturalist 136 (6), 829–846.
Winkler, A.M., Ridgway, G.R., Webster, M.A., Smith, S.M., Nichols, T.E., 2014. Permutation inference for the general linear model. Neuroimage 92, 381–397.
Zald, D.H., McHugo, M., Ray, K.L., Glahn, D.C., Eickhoff, S.B., Laird, A.R., 2014. Meta-analytic connectivity modeling reveals differential functional connectivity of the medial and lateral orbitofrontal cortex. Cereb. Cortex 24 (1), 232–248.